JOURNAL OF SOLID STATE CHEMISTRY 109, 241–250 (1994)

Lattice Vibration Spectra

LXXVIII.[1] Polymorphism and Phase Transitions of the Isostructural *M*SH (*M* = Na, K, and Rb)

K. Beckenkamp and H. D. Lutz

Universität Siegen, Anorganische Chemie I, D-57068 Siegen, Germany

and

H. Jacobs and U. Metzner

Universität Dortmund, Fachbereich Chemie, D-44227 Dortmund, Germany

Received March 29, 1993; in revised form July 9, 1993; accepted July 14, 1993

IR and Raman spectra (4000–50 cm^{-1}) of the isostructural alkaline metal hydrogensulfides *M*SH (*M* = Na, K, and Rb) as well as of deuterated specimens are recorded in the temperature range 10–540 K. The temperature evolutions of frequencies and halfwidths of the SH-stretching and librational modes clearly display the partly second-order phase transitions of the polymorphic title compounds. These phase transitions are driven by thermally activated disordering of the SH^- ions from the antiferroelectrically ordered low-temperature polymorphs (LTM) via the two-dimensionally disordered middle-temperature polymorphs (MTM) to three-dimensionally disordered high-temperature polymorphs (HTM). Because of the lack of full translational symmetry in the case of the disordered compounds IR and Raman bands are observed, which are not allowed by group theory. In the case of the LTMs, IR and Raman bands owing to disordered SH^- ions are observed additionally to the bands due to the ordered ions. With the exception of NaSH HTM, the SH^- ions are not involved in hydrogen bonds. This is revealed by both the SH-stretching frequencies, which are larger than that of free SH^- ions, and their negative temperature shifts.

INTRODUCTION

The hitherto only Raman spectroscopic investigation of the title compounds (1) suffers from the incomplete knowledge of the crystal structures of alkaline metal hydrogensulfides in the early seventies. In the meantime, detailed investigations on the crystal structures of the various polymorphs of these compounds (2–5) are available in addition to calorimetric (4–6), nuclear magnetic resonance (NMR) (7, 8), and inelastic and quasielastic neutron scattering investigations (9, 10). We therefore completed these studies by IR and Raman experiments of the isostructural *M*S(H, D) (*M* = Na, K, and Rb) in the temperature range 10–540 K in order to reveal bonding and orientational disorder of the SH^- ions as well as the mechanism of the phase transitions involved in more detail. Very recently Haines and Christy (11) reported on the pressure dependence of the IR and Raman bands of NaSH and KSH.

The low-temperature modifications (LTMs) of the title compounds crystallize in the monoclinic space group $P2_1/m$–C_{2h}^2 ($Z = 2$) with antiferroelectric ordering of the hydrogensulfide ions (3, 5) (see Fig. 1). At 113.5, 106.7, and 122.1 K (4, 6), respectively, the LTMs undergo order–disorder phase transitions to middle-temperature polymorphs (MTMs). They crystallize in the rhombohedric space group $R\bar{3}m$–D_{3d}^5 ($Z = 3$) with twofold orientationally disordered (parallel to the *c*-axis) SH^- ions (3, 5) (see Fig. 2). The MTMs disorder three-dimensionally to cubic high-temperature modifications (HTMs) (NaCl type, space group $Fm\bar{3}m$–O_h^5, $Z = 4$) (3, 5) at 360.7, 421.3, and 409.6 K, respectively (4, 6). The SH^- ions are aligned mainly parallel to ⟨110⟩. After D-NMR (7, 8) and neutron scattering experiments (9, 10) the SH^- ions rotate nearly quasi-freely. All phase transitions are indicated with only small changes in energy (5).

EXPERIMENTAL

The hydrogensulfides under investigation were prepared by reaction of the respective metals with liquid hydrogensulfide (H_2S, D_2S, etc.) at 320–420 K in an auto-

[1] Part LXXVII. M. Schmidt and H. D. Lutz, *Phys. Chem. Miner.* 20, 27 (1993).

0022-4596/94 $6.00

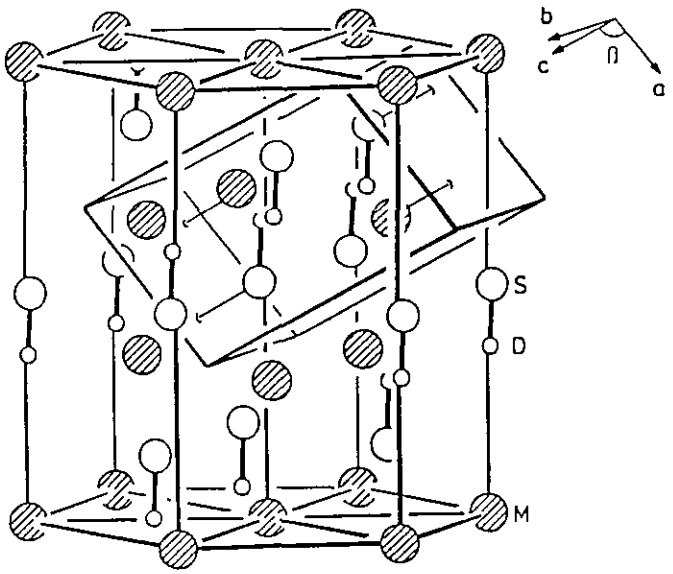

FIG. 1. Sketch of the crystal structure of the monoclinic low-temperature polymorphs of MSD (M = Na, K, and Rb) (pseudorhombohedral setting).

clave (3–6). The polycrystalline samples were loaded in glass capillaries under dry argon atmosphere to prevent decomposition reaction with moisture. All operations must be done in a glove box. The glass capillaries were annealed at 420 K for several weeks, slowly cooling down to ambient temperature in order to improve the crystallinity of the samples.

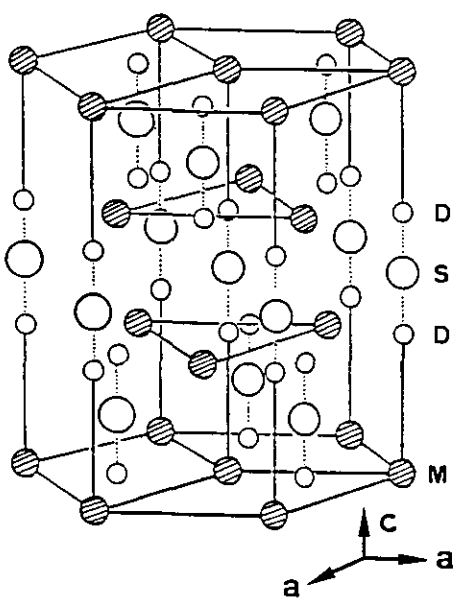

FIG. 2. Sketch of the crystal structure of the rhombohedral MTMs of NaSD, KSD, and RbSD.

TABLE 1

Unit-Cell Group (C_{2h}) Analysis of the Zone Center Phonon Modes of the Low-Temperature Polymorphs of the Isostructural MSH (M = Na, K, Rb)

Species	n	n_T	$n_{T'}$	n_R	n_i	Assignment
A_g	6	—	4	1	1	ν(SH), R_{ip}
A_u	3	1	1	1	—	R_{oop}
B_g	3	—	2	1	—	R_{oop}
B_u	6	2	2	1	1	ν(SH), R_{ip}

Note. n, total amount of irreducible representations; n_i, internal modes (SH-stretching vibrations, ν_{SH}); n_R, SH librations (R_{ip} and R_{oop}, in-plane and out-of-plane librations); $n_{T'}$, translational modes; n_T, translations.

The Raman spectra were monitored on an OMARS 89 multichannel Raman spectrograph (resolution <4 cm^{-1}) in the usual right-angle geometry. Further details in terms of the laser used and the laser power employed (to avoid light-induced decomposition), recording high- and low-temperature spectra (temperature accuracy ≈ 2 K), etc. are given elsewhere (12, 13). The IR spectra were recorded on a Perkin–Elmer model 580 spectrophotometer (resolution <1 cm^{-1}) using polychlortrifluorethen mulls on CsI plates (12).

The spectra were fitted with respect to the band shapes (both Gaussian and Lorenzian) in order to calculate the band energies, intensities, and half-widths using the program SPT (14). The half-widths (FWHM) of the Raman bands were fitted to a simple Arrhenius' law,

$$\ln(1/\Delta\nu_{1/2}) = V/(kT)^{-1} + C,$$

where $\Delta\nu_{1/2}$ values are the half-widths, V is the potential barrier, T the temperature, and k the Boltzmann constant. The correlation times τ are connected with the half-widths by $\Delta\nu_{1/2} = 1/\pi c\tau$ (where c is the velocity of light). For further details see (13, 15).

TABLE 2

Correlation of the SH-Stretching and Librational Modes of the Various Polymorphs of the Isostructural MSH (M = Na, K, Rb)

Free SH^- ion		Site groups			Unit-cell group	
	$C_{\infty v}$	C_{2v}(HTM)	C_{3v}(MTM)	C_s(LTM)	C_{2h}(LTM)	
ν(SH)	Σ	A_1	A_1	A'	A_g	ν(SH), R_{ip}
					A_u	R_{oop}
$R_{x,y}$	Π	B_1	E	A''	B_g	R_{oop}
		B_2			B_u	ν(SH), R_{ip}

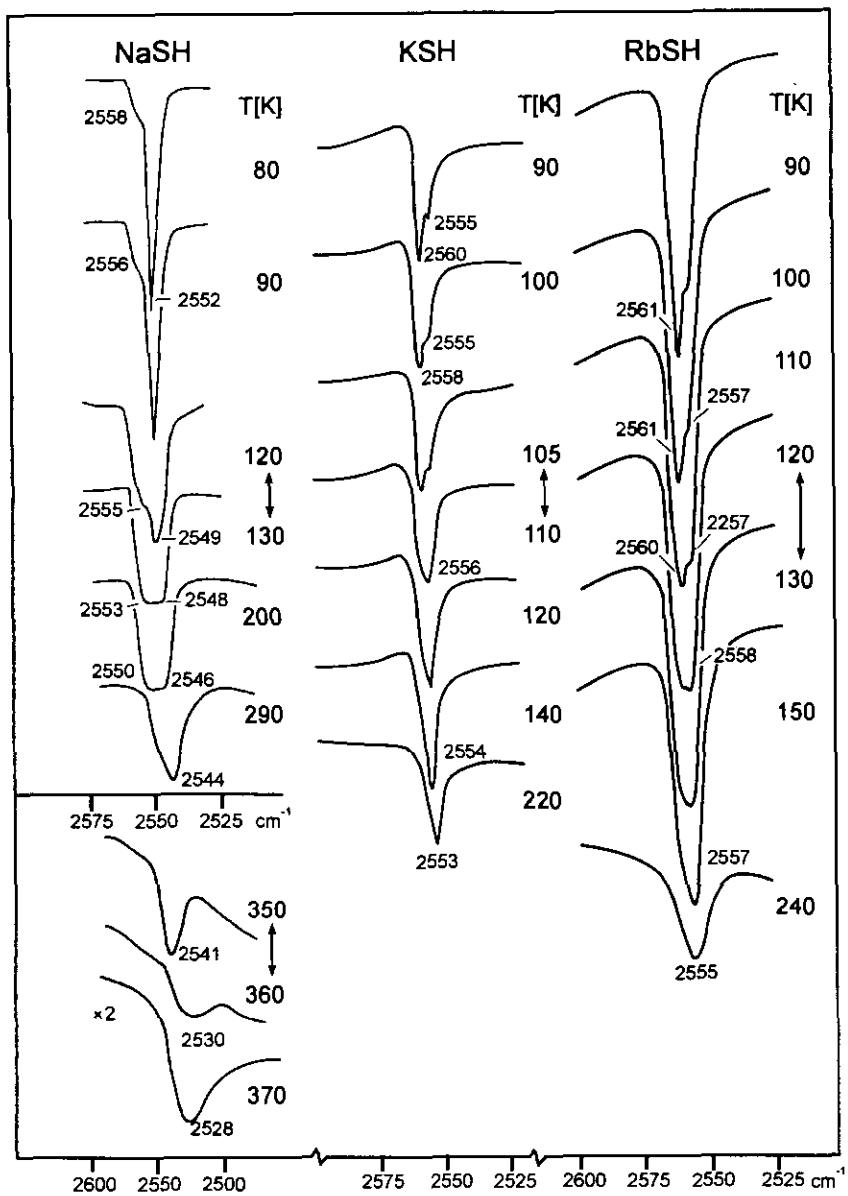

FIG. 3. IR spectra of NaSH, KSH, and RbSH in the SH-stretching mode region (arrows, phase transitions).

GROUP-THEORETICAL TREATMENT OF THE IR AND RAMAN BANDS

The monoclinic low-temperature polymorphs of the title compounds display one SH-stretching mode, two SH librations, and six and three translational modes in the Raman and IR spectra, respectively, (unit-cell group C_{2h}, see Table 1). For the other polymorphs, group theoretical treatment of the external vibrations is more complicated because of the orientational disorder of the hydrogensulfide ions.

In the case of the MTMs (unit-cell group D_{3d}), two IR-allowed translational modes ($\Gamma = A_{2u} + E_u$), one degenerated SH libration (site group C_{3v}, $\Gamma = E$) and one SH-stretching mode ($\Gamma = A_1$), which are both IR and Raman allowed, are expected (see Table 2). However, because of the breakdown of the full translational symmetry caused by the orientational disorder of the SH^- ions, additional bands may be present due to antiphase vibrations of ions of adjacent unit cells, e.g., Raman-allowed translational modes or more than one SH librations. In the case of the HTMs (unit-cell group O_h), one IR-allowed lattice mode (species F_{1u}) and one SH-stretching mode (species A_1 of the site group C_{2v}), which is both IR and Raman allowed, are expected. Additional bands may be observed due to the loss of the full translational symmetry

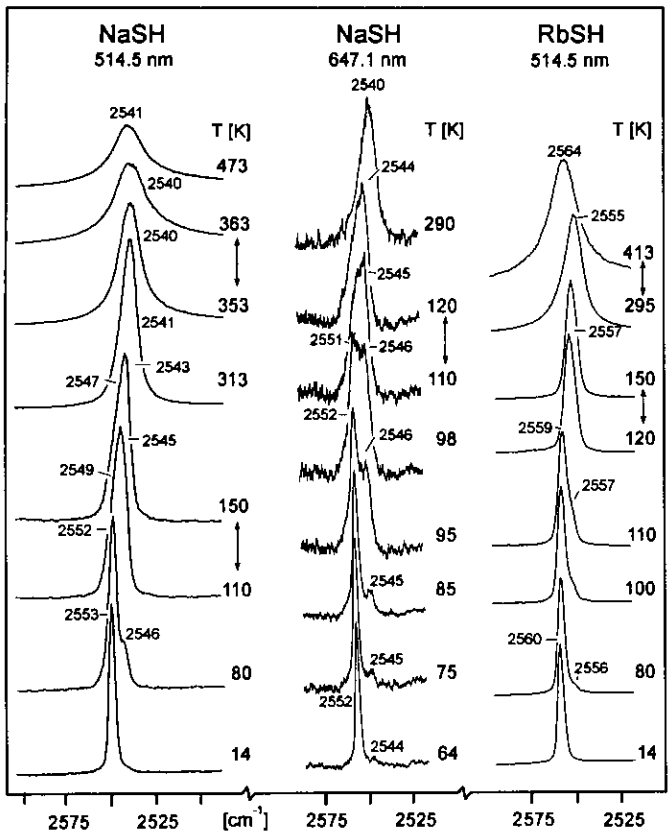

FIG. 4. Raman spectra of NaSH and RbSH in the SH-stretching mode region (excitation 514.5 and 647.1 nm, respectively; arrows, phase transitions).

and the possible presence of SH^- ions with C_{3v} site symmetry, i.e., SH^- ions orientated parallel to ⟨111⟩ (additional to those parallel to ⟨110⟩). The observation of SH librations depends on the residence time of the hydrogen atoms at the respective split positions (15).

RESULTS

IR and Raman spectra of the title compounds are shown in Figs. 3–7. The bands observed are assigned as given in Table 3. The Raman spectra of NaSH obtained resemble those reported by Rush *et al.* (1).

1. SH- (and SD) Stretching Modes

The isotopically dilute samples (i.e., samples deuterated by about 6 and 95%, respectively) display only one SD- resp. SH-stretching mode in both the Raman and IR spectra in the case of all polymorphs of the title compounds as predicted by group theory (see Fig. 5 and Table 3).

The temperature evolution of the energies and half-widths (FWHM) of the bands under discussion reveals the phase transitions of the alkaline hydrogensulfides studied (see Fig. 8). The transition temperatures obtained correspond to those recorded by DSC experiments within 2 K. These phase transitions are also shown from the temperature evolution of the SH-stretching modes of the neat compounds (see Figs. 3–5, and 9). On going from the LTMs to the MTMs the SH modes are shifted to smaller wavenumbers by 5–6 cm^{-1}. With the exception of the sodium compound, the band frequencies increase again in connection with the phase transition to the HTMs. The temperature dependence of the SH-stretching modes within the stability regions of the three hydrogensulfide polymorphs is negative ($d\nu(SH)/dt < 0$). The half-widths of the bands increase with the increase in temperature (see Fig. 8).

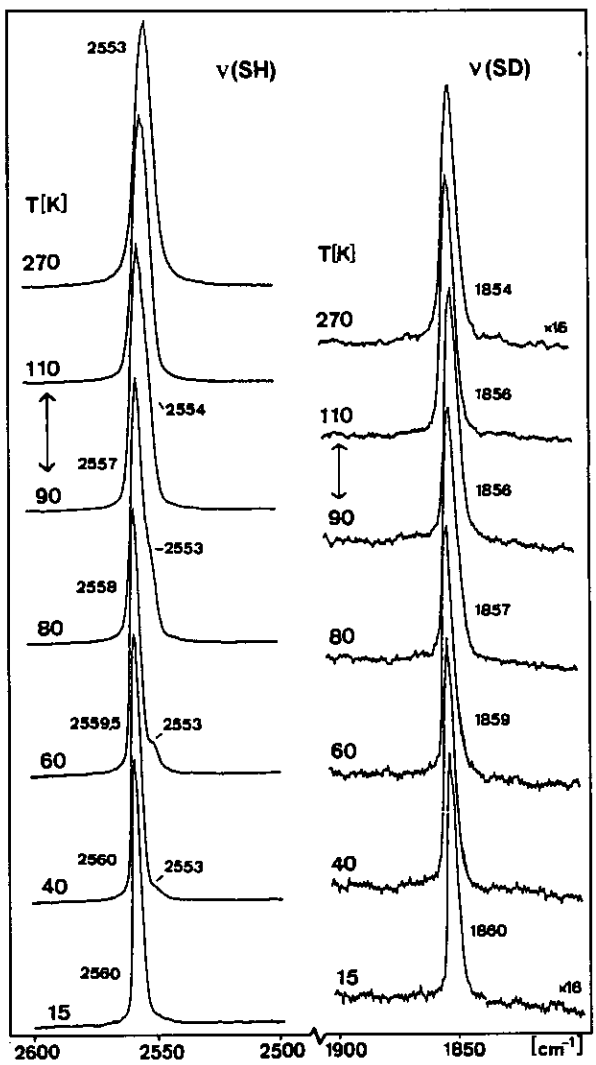

FIG. 5. Raman spectra of KS(H, D) in the SH- (neat compound) and SD- (isotope dilute sample) stretching mode region (excitation 514.5 nm; arrow, phase transition LTM to MTM).

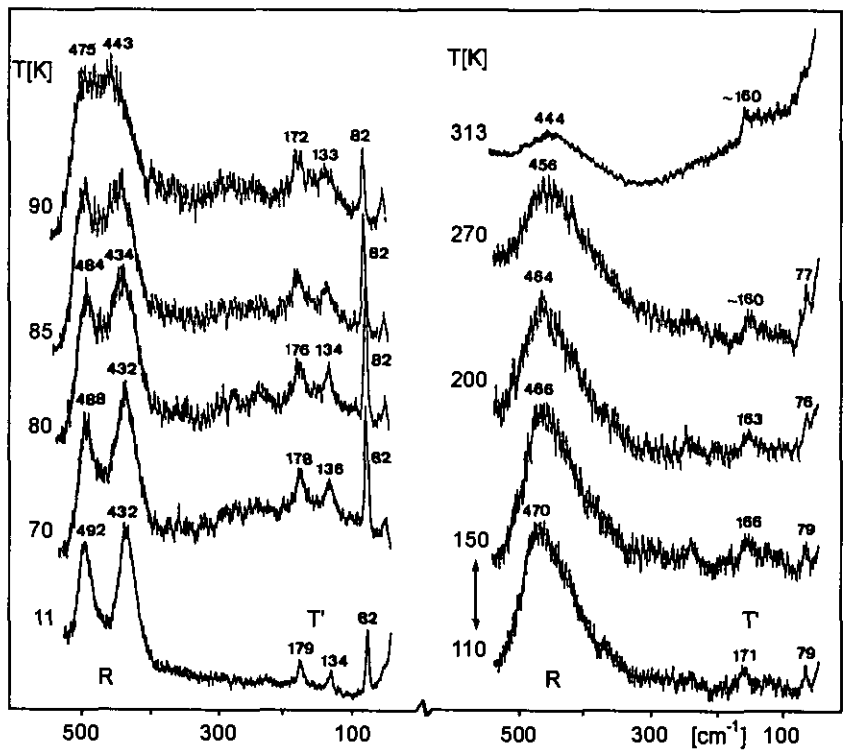

FIG. 6. Raman spectra of NaSH in the SH librational (R) and translational mode (T') region (excitation 514.5 nm; arrow, phase transition LTM to MTM).

The SH-stretching modes of the neat compounds are likewise observed in both the Raman and IR spectra as predicted from the site symmetry of the SH^- ions in the various *M*SH polymorphs as discussed above. The frequencies of the respective IR and Raman bands are equal within the range of experimental error (<3 cm^{-1}) corresponding to those of the uncoupled SH modes (see Table 3). However, some additional bands are observed in the spectra of the LTMs (see Figs. 3–5).

In the case of KSH and RbSH, a low-energy shoulder of the SH-stretching mode is observed in both the IR and Raman spectra. The intensities of these additional bands increase with increasing temperature; the frequency differences to the main band decrease from 8 and 5 cm^{-1} below 80 K to <2 cm^{-1} at the transition temperatures to the MTMs. In the case of NaSH, these shoulders are different in the IR and Raman spectra, i.e., there is an additional high-energy mode in the IR spectra and a low-energy shoulder in the Raman spectra (see Figs. 3 and 4). The frequency difference of these shoulders decreases with the increase in temperature from 14 cm^{-1} at 70 K to <8 cm^{-1} near the phase transition to the MTM (see Fig. 9). The intensities of both additional bands increase with increasing temperature in a way similar to that found for KSH and RbSH. The high-frequency IR band is maintained in the MTM.

2. *Librations of SH^- and SD^- Ions*

The SH librations of the isostructural NaSH, KSH, and RbSH, which can be assigned from their H/D isotopic shifts of ≈1.40, display different behavior (see Figs. 6 and 7). Whereas the two librations predicted by group theory, i.e., the in-plane and the out-of-plane librations, R_{ip} and R_{oop}, (see Tables 1 and 2), coincide in the LTMs and the MTMs of both KSH and RbSH, these bands are different in energy for the LTM of NaSH (see Fig. 10) by up to 60 cm^{-1}. This splitting of the librations reflects the amount of the monoclinic distortion of the LTMs, which is much greater for NaSH than for KSH and RbSH (5). The assignment of the librational modes given, viz., $R_{oop} > R_{ip}$, is based on the different repulsive proton–proton interactions for these vibrations. (The unit-cell group splittings of R_{ip} and R_{oop}, i.e., those of the respective IR and Raman bands, are negligible.) The librational mode energies range as NaSH (mean value) ≫ KSH > RbSH owing to the decreasing cohesive energy in this order.

In the case of the LTMs, the frequencies of the SH librations increase with the increase in temperature, but they decrease for the MTMs (see Fig. 10). The highest frequencies are monitored at the temperatures of the phase transition of the LTMs to the MTMs. In the course of the phase transition to the HTMs, there is no significant

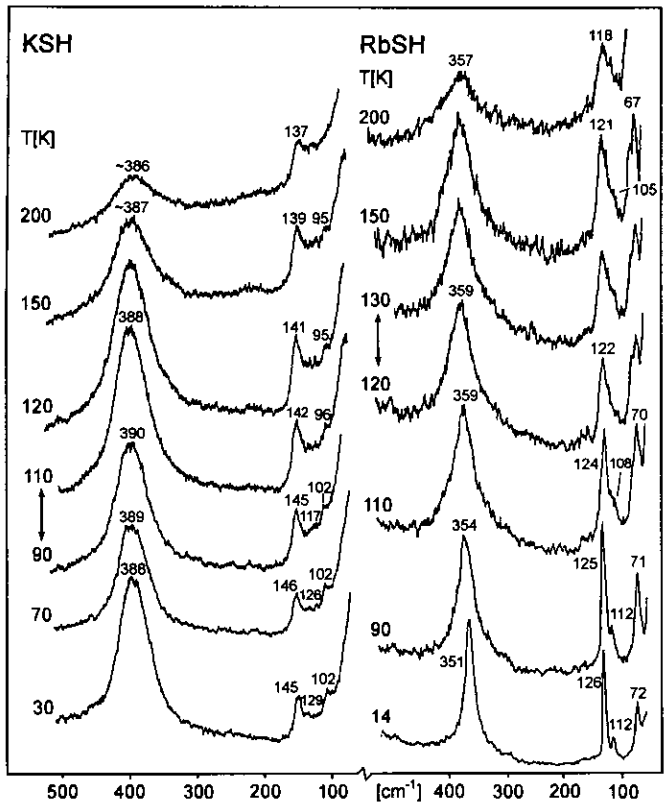

FIG. 7. Raman spectra of KSH and RbSH in the external mode region (R(SH), T') (514.5 nm; arrows, phase transitions LTMs to MTMs).

shift of the SH librations. However, only in the case of NaSH, a broad band due to SH librations was detected.

3. *Translational Vibrations*

In the case of the LTMs, three of the six translational modes allowed by group theory are observed in the Raman spectra as shown in Figs. 6 and 7. The frequencies of the two high-energy bands range as NaSH > KSH > RbSH, as expected from the decreasing masses of the alkaline metal ions involved. The relative intensities of the highest frequency lattice modes increase on going from the sodium to the rubidium compound, which results from the increase of the polarizabilities of the respective metal ions.

The phase transitions to the MTMs are revealed by the strong increase of the half-widths of the two remaining Raman bands, i.e., the highest and lowest energy modes. These two bands, which are not allowed by group theory, at least in the case of preservation of the full translational symmetry (see above), are interpreted as being owing to density-of-states maxima of the transversal optical lattice vibrations of the SH^- ions (1, 9).

4. *Dynamics of the Reorientation of the SH^- Ions*

The activation energies, V, activation temperatures, V/k, correlation times, τ, etc., which are calculated from the temperature evolution of the half-widths of the observed bands (see above), are given in Table 4. The potential barriers, V, for reorientation of the SH^- ions of the MTMs decrease on going from the sodium to the rubidium compound. The correlation times are in the order of 1–4 ps (MTMs), <1 (HTMs) for ν(SH) and <0.1 ps (MTMs) for R(SH). They range as NaSH < KSH < RbSH (ν(SH)) decreasing with the increase in temperature.

DISCUSSION

1. *Bonding of the SH^- Ions*

The SH^- ions of the hydrogensulfides under investigation are not involved in hydrogen bonds (with the exception of NaSH HTM, see below). This is shown from the respective S···S distances, which are larger than 380 pm for all polymorphs of the title compounds (5), and from both the SH-stretching frequencies, which are greater than 2540.5 cm^{-1}, the band frequency of free, gaseous hydrogensulfide ions (16), and the negative temperature shifts of these vibrations (13).

The frequencies of the SH-stretching modes range as NaSH $\ll$ KSH $\approx$ RbSH (see Table 3 and Fig. 9). This order is unexpected. As a result of stronger polarization of the S–H bond by the smaller Na^+ ions than by the bigger Rb^+ and K^+ ions, this order should be reversed in a way similar to that found for solid hydroxides (17). The higher frequencies of the SH-stretching modes of KSH and RbSH compared to that of NaSH, however, are very probably caused by repulsion effects. These repulsion forces are in the order NaSH $\ll$ KSH < RbSH, which is the same sequence as found for the SH-stretching modes, which increase in frequency with the increase of the repulsion forces at the respective lattice sites. These repulsion forces overcompensate the hardening of the modes owing to the polarization of the SH bonds.

The order of repulsion mentioned above is related to the decreasing nearest "open" metal–metal distances derived from the experimental $M\cdots M$ distances by correction for the ionic radii. They are 156 (= 388 − 2 × 116), 125 (= 429 − 2 × 152), and 111 (= 443 − 2 × 166) pm, respectively, for the LTMs of the title compounds (the $M\cdots M$ distances are from (5) (see Fig. 11) and the ionic radii are from (18)). These repulsion forces of the metal ions are probably also the reason for the amount of the rhombohedral distortion of the lattice connected with the HTM-to-MTM phase transition, a question that was discussed by Teichert and Klemm in 1939 (19).

TABLE 3
Assignment of the SH- and SD-Stretching Modes and Librations of the Isostructural NaSH, KSH, and RbSH (cm^{-1})

Temperature (K)	NaSH IR	NaSH Raman	KSH IR	KSH Raman	RbSH IR	RbSH Raman	Assignment
			Low-temperature polymorphs (LTM, *mP*6)				
90	2556	2546	2555	2554	2557	2557	ν(SH), MTM
	2551	2551	2560	2558	2561	2560	ν(SH), A_g, B_u
			2560		2559		ν(SH)[1]
	1852	1851		1856	1854		ν(SD), A_g, B_u
		1852	1858	1856	1855		ν(SD)[1]
	470	475		390	365	354	R_{oop}(SH)
	445	443		390	365	354	R_{ip}(SH)
	≈340			280		254	R_{oop}(SD)
	316			280		254	R_{ip}(SD)
			Middle-temperature polymorphs (MTM, *hR*3)				
150	2553		2554	2554	2557	2557	ν(SH), A_1
	2547	2547					
		2546					
		2546		2555		2555	ν(SH)[1]
				1853		1855	ν(SD), A_1
		1851		1853		1855	ν(SD)[1]
		466		387		359	R(SH), E
300	2544	2542	2553	2553	2556	2555	ν(SH), A_1
		2545				2555	ν(SH)[1]
		1849		1852		1856	ν(SD), A_1
		1850	1852	1852		1855	ν(SD)[1]
		≈450		≈384		≈350	R(SH), E
		≈320				≈246	R(SD), E

[1] Matrix-isolated SH^- and SD^- ions present in samples deuterated by 6 and 94%, respectively.

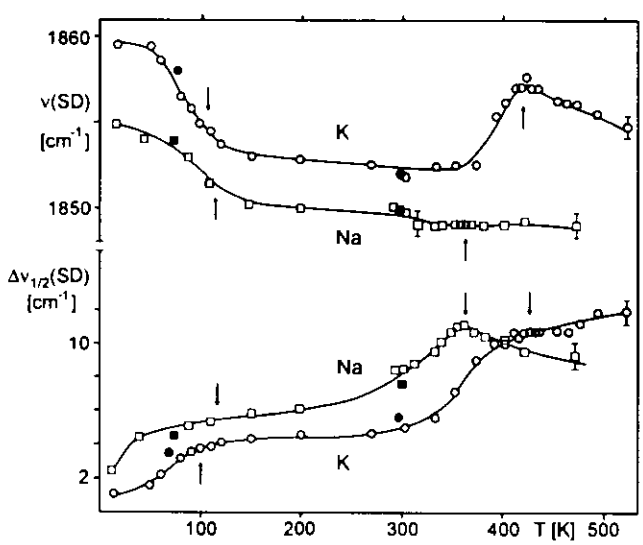

FIG. 8. Temperature evolution of the frequencies (ν(SD)) and half-widths ($\Delta\nu_{1/2}$) of the stretching modes of matrix-isolated SD^- ions (6% D) in NaS(H, D) and KS(H, D) (□, ■, NaSH; ○, ●, KSH; closed symbols, IR bands; open symbols, Raman bands; arrows, phase transitions).

2. *Disorder of the SH^- Ions*

The additional SH-stretching modes in the LTMs of KSH and RbSH, which are observed at temperatures above 40 K (see Figs. 3–5, 8, and 9) increasing in intensity with increasing temperature, must be assigned to SH^- ions which are disordered as in the MTMs of these compounds. The small differences in frequency of the stretching modes of ordered and disordered SH^- ions are owing to the long-range antiferroelectrical ordering of the ordered ions.

The disordered SH^- ions present in the LTM of NaSH, on the other hand, display two additional bands, i.e., a high-energy Raman band and a low-energy IR absorption peak, each beside the main band of the ordered LTM (see above). These bands behave with respect to temperature increase similarly to the analogous bands of KSH and RbSH. The mean values of the frequencies of these bands equal those of uncoupled SH-stretching modes (isotopically dilute SH^- ions).

The two additional bands of NaSH LTM result from a coupling of the vibrations of disordered SH^- ions of adjacent unit cells, which are antiferroelectrically oriented

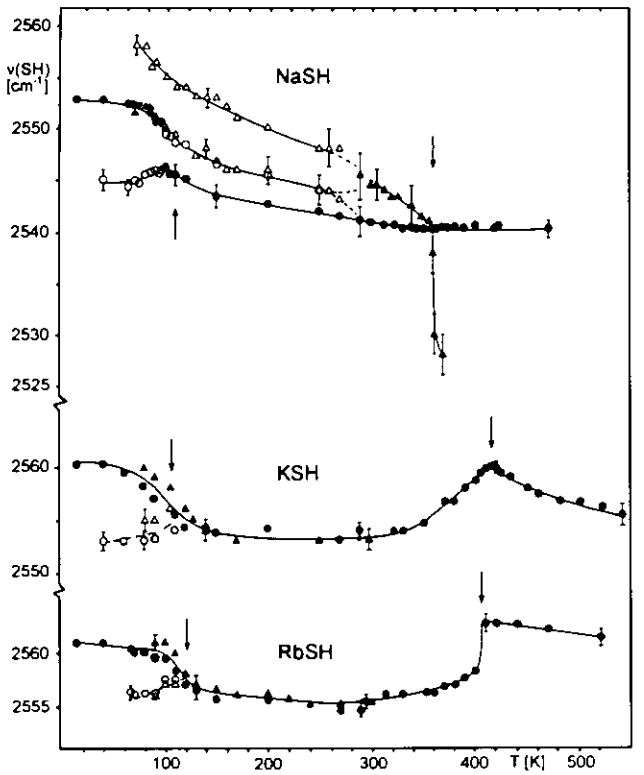

FIG. 9. Temperature evolution of the SH-stretching mode frequencies of MSH (M = Na, K, Rb) (neat compounds) (○, ●, Raman bands (mean values of 514.5- and 647.1-nm excitation), △, ▲, IR bands; open symbols shoulders; arrows, phase transitions).

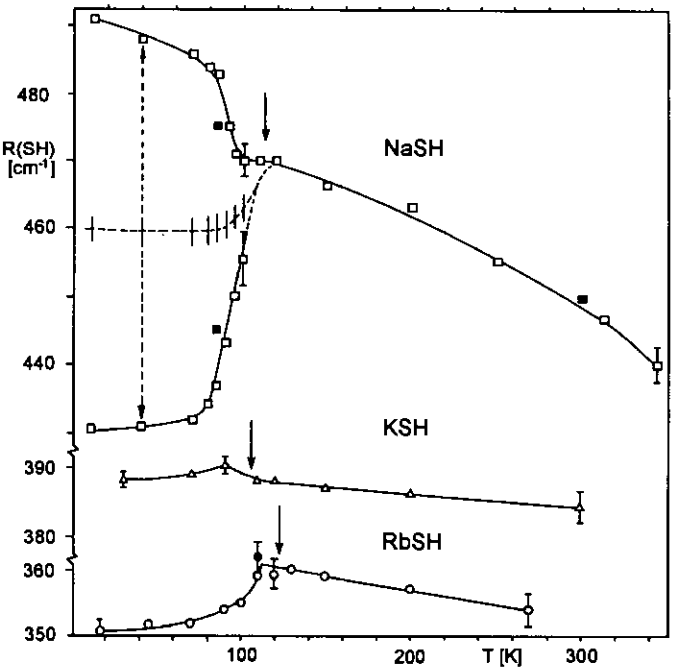

FIG. 10. Temperature evolution of the SH librations of the isostructural MSH (□, ■, NaSH (|, mean values of the two modes); △, KSH; ○, ●, RbSH; closed symbols, IR bands; open symbols, Raman bands; arrows, phase transitions).

within the *ac* plane of the structure instead of the ferroelectric ordering in the ordered structure (see Fig. 11), yielding a Raman-allowed band (in-phase vibrations) and an IR-allowed one (antiphase vibrations). The distance of the ferroelectrically oriented ordered SH^- ions ($SH^0 \cdots SH^0$) is similar (391 pm) to that of the antiferroelectrically oriented SH^- ions within the unit cell ($SH^0 \cdots SH^1$) (388 pm). (In the case of KSH and RbSH, the respective interionic S···S distances are too large (>430 pm) for such couplings.) This vibrational coupling of the disordered SH^- ions in the *ac* plane, which is affected by strong dipole–dipole interactions, produces the great frequency splittings observed. The decrease of this splitting with the increase in temperature is due to the increasing disordering dynamics. The observed vibrational coupling of the disordered SH^- ions supports the cooperative reorientational motions of the SH^- ions concluded from the results of NMR experiments (7).

3. *Mechanism of the Phase Transitions*

The partly second-order phase transitions of the ordered LTMs to the two-dimensionally disordered MTMs of the title compounds, which are driven by the thermically activated orientational motions of the SH^- ions (gain of additional entropy), are shown by the intensity increase of the additional SH-stretching modes discussed above (see Figs. 3–5 and 12). The temperature-dependent equilibria between ordered and disordered SH^- ions thus established enable the respective energies, ΔH^0, and entrop-

TABLE 4

Potential Barriers (V), Activation Temperatures (V/k), and Correlation Times (τ) of the Reorientational Motions of the SH^- Ions in the Mean-Temperature Polymorphs of the Isostructural NaSH, KSH, and RbSH Derived from the Temperature Dependence of the Half-Widths of the SH-Stretching Modes and Librations ν(SH) and R(SH)

	Temperature range (K)	V (kJ mol^{-1})	V/R (K)	r	τ (ps)	Temperature (K)
			(SH)			
NaSH	110–323	0.1(1)	9(5)	0.800	1.5	(200)
	323–363	24.0(50)	2886(600)	0.960	0.9	(350)
KSH	323–408	8.3(1)	998(50)	0.996	1.1	(350)
RbSH	313–408	7.3(10)	881(100)	0.994	1.5	(350)
			R(SH)			
NaSH	110–270	0.1(1)	11(6)	0.958	0.1	(200)
KSH	110–200	0.4(1)	47(10)	0.997		
RbSH	110–270	1.0(3)	120(40)	0.952		

Note. r, straight line correlation coefficient; R, gas constant.

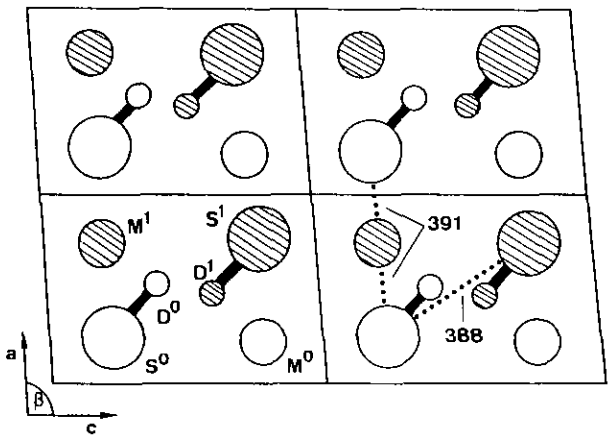

FIG. 11. Projection of the crystal structure of the low-temperature polymorphs of MSH (M = Na, K, Rb) on the ac plane (101) (open circles, y = 1/4; hatched circles, y = 3/4; distances, pm).

ies, ΔS^0, involved to be calculated by the use of the equation

$$\ln I = -\Delta H^0/RT + \Delta S^0/R,$$

where I is the relation of the integral scattering intensities of the disordered and the ordered SH^- ions. The data obtained are 4.8(1) and 5.0(4) kJ mol^{-1}, and 4.5(5) $\times$ 10^{-2} and 3.7(4) $\times$ 10^{-2} kJ mol^{-1} K^{-1} for NaSH and RbSH, respectively (12). The temperatures, at which $\ln I = 0$, i.e., 113 and 122 K for NaSH and RbSH, respectively, correspond to the phase transitions to the MTMs.

The phase transitions from the MTMs to the HTMs start at temperatures <300 K, which is revealed from

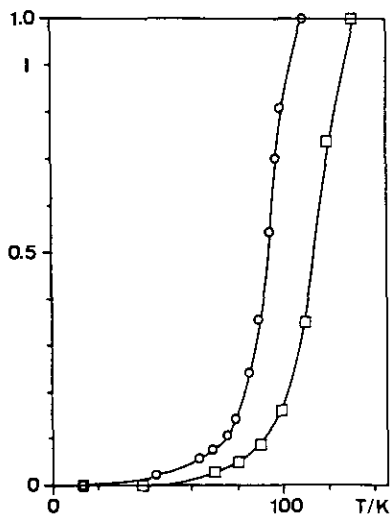

FIG. 12. Temperature evolution of the intensity relations I of the SH-stretching mode Raman bands of disordered and ordered SH^- ions in the low-temperature polymorphs of NaSH (○) and RbSH (□).

the unexpected increase of the frequencies of the SH-stretching modes (at least in the case of KSH and RbSH) with increasing temperature (see Figs. 8 and 9). (This beginning of the three-dimensionally disordering of the SH^- ions is also shown from the course of the specific heats (4, 19) of the hydrogensulfides under investigation.) The continuous transitions from the MTMs to the HTMs occur via partial occupation of the energetically unfavorable pseudo ⟨111⟩ axes of the rhombohedrically distorted $M(SH)_6$ octahedra of the MTMs by disordered SH^- ions. Because of the stronger $M\cdots H$ repulsion at these positions the SH-stretching modes are hardened increasingly with the increase in temperature. Not only if the ⟨111⟩ axes (or the ⟨110⟩ ones in the case of C_{2v} sites (5), see above) are equivalent in the cubic HTMs the frequencies of the SH modes decrease with the increase in temperature.

In the case of the MTM of NaSH, this frequency increase is not observed. The phase transition to the HTM is signalized by a frequency crossing of the respective IR and Raman bands (see Fig. 9). These findings reveal that the transition mechanism is different from that of KSH and RbSH. Thus, the frequency crossing of the IR and Raman bands may be interpreted with the change of the main orientation of the SH^- ions from ⟨111⟩ in the pseudo-cubic MTM to ⟨110⟩ in the HTM.

The SH-stretching modes of NaSH HTM are observed in the IR spectra at ≈2530 cm^{-1} (above 370 K), i.e., below that of free SH^- ions (2540.5 cm^{-1} (16)), and in the Raman spectra at ≈2540 cm^{-1}. Therefore, a coupling of SH^- motions may be taken into account resembling weak hydrogen bonds. This assumption is reasonable because the protons are oriented to adjacent sulfur atoms (contrary to SH ions aligned parallel to the ⟨111⟩ axes) and the corresponding $S\cdots S$ distances are relatively short (428 pm (5)). Ordinary $SH^-\cdots SH^-$ hydrogen bonds have only been established for CsSH LTM (12) with CsCl-type structure and $d(S\cdots S)$ = 418 pm (6). The corresponding $S\cdots S$ distances of KSH and RbSH are too long for forming H-bonds and, hence, such bonds are not observed in the spectra.

CONCLUSION

In this work, the polymorphism and the phase transitions of the isostructural alkaline metal hydrogensulfides NaSH, KSH, and RbSH have been studied by infrared and Raman spectroscopic experiments. Both frequencies and half-widths of the SH-stretching and librational modes, especially their temperature evolutions, are powerful tools for determination of the structural environments and the dynamic behavior of the SH^- ions. This is possible even though the breakdown of the full translational symmetry due to the disordering of the SH^- ions does not enable complete group-theory treatments. The

phase transitions from ordered polymorphs at low temperatures via two-dimensionally disordered middle-temperature modifications to three-dimensionally disordered, cubic high-temperature polymorphs are partly second order in nature. They result from a thermally driven disordering of the SH^- ions. The absence of hydrogen bonding in the case of most phases being studied is displayed by both the relatively large S···S distances and SH-stretching frequencies greater than that of free SH^- ions, i.e., 2540.5 cm^{-1}.

REFERENCES

1. J. J. Rush, R. C. Livingston, and G. J. Rosasco, *Solid State Commun.* **13,** 159 (1973).
2. L. W. Schroeder, L. A. De Graaf, and J. J. Rush, *J. Chem. Phys.* **55,** 5363 (1971).
3. U. Metzner, PhD thesis. University of Dortmund, Germany, 1989.
4. H. Jacobs and C. Erten, *Z. Anorg. Allg. Chem.* **473,** 125 (1981).
5. H. Jacobs, U. Metzner, R. Kirchgässner, H. D. Lutz, and K. Beckenkamp, *Z. Anorg. Allg. Chem.* **598/599,** 185 (1991).
6. R. Kirchgässner, PhD Thesis. University of Dortmund, Germany, 1988.
7. K. R. Jeffrey, *Can. J. Phys.* **52,** 2370 (1974).
8. K. R. Jeffrey and R. E. Wasylishen, *Can. J. Phys.* **59,** 1585 (1981).
9. J. J. Rush, L. A. De Graaf, and R. C. Livingston, *J. Chem. Phys.* **58,** 3439 (1973).
10. J. M. Rowe, R. C. Livingston, and J. J. Rush, *J. Chem. Phys.* **58,** 5469 (1973).
11. J. Haines and A. G. Christy, *Phys. Rev. B* **46,** 8797 (1992).
12. K. Beckenkamp, PhD thesis. University of Siegen, Germany, 1991.
13. K. Beckenkamp, H. D. Lutz, H. Jacobs, and U. Metzner, *J. Mol. Struct.* **245,** 203 (1991).
14. W. Langel, "Program SPT for Band Shape Analysis." University of Siegen, Germany, 1989.
15. G. Schaak, *J. Mol. Struct.* **79,** 361 (1982).
16. M. Gruebele, M. Polak, and R. J. Saykally, *J. Chem. Phys.* **86,** 1698 (1987).
17. K. Beckenkamp and H. D. Lutz, *J. Mol. Struct.* **270,** 393 (1992).
18. R. D. Shannon, *Acta Crystallogr., Sect. A* **32,** 751 (1956).
19. W. Teichert and W. Klemm, *Z. Anorg. Allg. Chem.* **243,** 86 (1939).